On the accuracy and robustness of implicit LES / under-resolved DNS approaches based on spectral element methods

Rodrigo C. Moura, Joaquim Peiró, Spencer J. Sherwin

Department of Aeronautics, Imperial College London
Prince Consort Rd, London, SW7 2BY, UK
r.moura13@imperial.ac.uk

ABSTRACT

We present a study on the suitability of under-resolved DNS (uDNS) – also called implicit LES (iLES) – approaches based on spectral element methods (SEM), with emphasis on high-order continuous and discontinuous Galerkin (i.e. CG and DG) schemes. Broadly speaking, these are model-free eddy-resolving approaches to turbulence which solve the governing equations in unfiltered form and rely on numerical stabilization techniques for small-scale regularization. Model problems in 1D, 2D and 3D are used in the assessment of solution quality and numerical stability. A rationale for the excellent potential of these methods for transitional and turbulent flows is offered on the basis of linear dispersion-diffusion analysis.

INTRODUCTION

SEM-based uDNS / iLES approaches have received significant attention over the last few years (Uranga *et al.*, 2011; Beck *et al.*, 2014; Vermeire *et al.*, 2016; Fernandez *et al.*, 2017). In some cases, these have been shown to outperform classic LES approaches with sophisticated modelling and provide superior results for the same number of DOFs, see e.g. (Gassner & Beck, 2013; Lombard *et al.*, 2016). However, very few studies have investigated the question of why these methods are able perform so well. Moreover, it is important to explore under which conditions they can fail to produce usefully accurate solutions or even "crash" due to under-resolution. As SEM approaches differ depending on design variables such as discretization order, Riemann solver, polynomial dealiasing and alternative stabilization strategies, it is crucial to analyse the effect of these variables on solution quality and numerical robustness.

As SEM-uDNS relies on stabilization techniques such as upwind dissipation for DG (Moura *et al.*, 2015*b*) or spectral vanishing viscosity for CG (Moura *et al.*, 2016*b*) in lieu of subgrid-scale models, the assessment of numerical diffusion effects is of key importance in understanding why and how to use these methods. Note that traditional iLES approaches (Grinstein *et al.*, 2007) justify their suitability by comparing truncation errors of candidate schemes to known LES models. Modified equation analysis has been employed to show that the leading truncation terms of certain schemes resemble mixed subgrid-scale models (Margolin & Rider, 2002). As this seems unlikely to hold for high-order SEM (Moura *et al.*, 2015*a*), the terminology under-resolved DNS is preferred here. In the next section, a case will be made that the suitability of SEM-uDNS stems primarily from the fact that dissipation is only significant at small flow scales. Interestingly, this is also the main property that traditional iLES approaches seek (Margolin & Rider, 2005).

Insights about the distribution of dissipation across scales can be obtained from linear dispersion-diffusion analyses, whose relevance to under-resolved simulations has been discussed in (Moura *et al.*, 2015*b*). There, a simple criterion to estimate DG's resolution power was proposed and tested against Burgers turbulence in 1D. This criterion was recently adapted with success to 3D flows (Moura *et al.*, 2017). The present paper discusses these results and new ones obtained with CG for vortex-dominated flows in 2D.

BURGERS TURBULENCE IN 1D

Numerical experiments on Burgers turbulence in one dimension have been conducted with DG by Moura *et al.* (2015*b*). The inviscid Burgers equation was simulated in a periodic setting with a forcing term that granted a Kolmogorov-like slope on the inertial range of the energy spectrum. Due to the absence of viscosity, DG's upwind dissipation is the only source of diffusion present. The dissipation characteristics obtained from DG's dispersion-diffusion analysis for linear advection are shown in Fig. 1. It basically shows a plot of (normalized) dissipation vs. (normalized) wavenumber for various discretization orders.

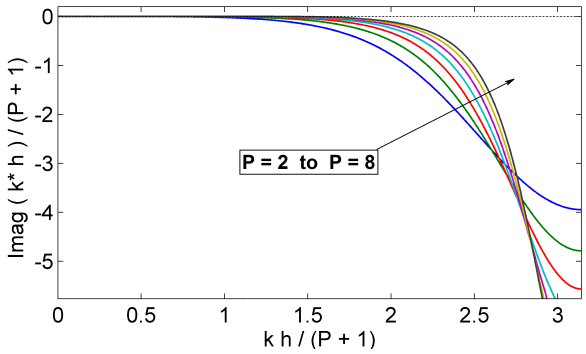

Figure 1. DG's numerical diffusion vs. wavenumber $kh/(p+1)$, with h being the mesh spacing and p the polynomial order.

In the simulations, several polynomial orders p have been considered on a fixed DOF basis, where $n_{DOF} = n_{e\ell}\, m$, with $m = p+1$ being the number of polynomial modes per element and $n_{e\ell}$ the total number of mesh elements. Therefore, larger p were assigned to smaller $n_{e\ell}$ and vice-versa, so that discretizations of different orders are compared at a similar cost measure. Note that Fig. 1 also compares different orders on a same DOF basis, since $h \propto 1/n_{e\ell}$.

A high-order solution is compared to a low-order one in Fig. 2, which shows that using larger p with coarser grids is beneficial given the wider range of scales captured. This is consistent with Fig. 1, as higher orders are shown to yield a larger dissipation-free wavenumber range. A measure of spectral resolution power based on the extent of this dissipation-free range has been proposed in (Moura *et al.*, 2015*b*) and shown to accurately pinpoint the beginning of a numerically-induced dissipation range on energy spectra.

The success of the estimates mentioned above indicates that linear dispersion-diffusion analysis can in fact provide insights on the suitability of spectral element methods (DG in particular) for under-resolved turbulence simulations. It seems that DG's high-order upwind dissipation is negligible for a reasonably large range of wavenumbers, beyond which it rises sharply. In this sense, the advocated methodology is similar to a direct numerical approach where hyperviscosity is used to truncate the energy spectrum (Lamballais *et al.*, 2011; Dairay *et al.*, 2017). If truncation is placed well within the inertial range, large scales can be faithfully represented.

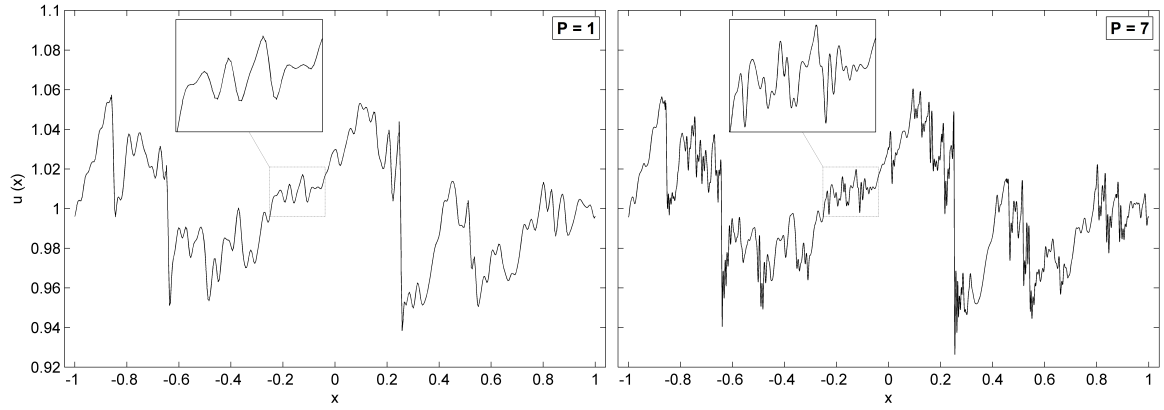

Figure 2. Burgers turbulence at a given time, comparing second-order (left) and eight-order (right) solutions with same DOFs.

VORTEX-DOMINATED FLOWS IN 2D

This section is devoted to numerical experiments conducted with CG on two-dimensional vortical flows. Emphasis is placed on the effects of mesh coarsening upon wake structures. Since mesh spacing is typically increased along turbulent wakes in simulations, it is important to assess the effects of this practice in the accuracy and stability of computations. The problem considered is that of a flow in a channel (with free-slip walls) where a cross-flow screen is placed before the inlet of the domain, see Fig. 4.

With the appropriate inflow conditions, instabilities develop soon after the inlet and a turbulent-like vortical state sets in. Wake structures are then carried away by the mean flow and leave the domain through an outlet, where outflow boundary conditions are applied. The main test case to be discussed here had a domain composed of two parts. One of them covered the first 60% of the domain and had an equispaced mesh of square-shaped elements. The remaining part had a mesh with six times less elements in the streamwise direction, but the same cross-flow distribution of elements. This amounted to an increase factor of four in the streamwise mesh spacing for the domain's second part. Fifth-order polynomials ($p = 5$) have been used in all the elements.

The distribution of streamwise velocity of a CG-based incompressible flow solution is depicted in Fig. 4. Note that small-scale features quickly disappear after 'station 60%', since the largest wavenumber one can hope to capture given p is inversely proportional to the mesh spacing h (Fig. 1). This test case has a Reynolds number of $3 \cdot 10^4$, based on the inflow length scale and (unit) mean velocity. Decreasing the viscosity caused the simulation to crash after a certain time. Spectral analysis indicated a build-up of small-scale energy prior to station 60%, as shown in Fig. 5, which was found to be the primary cause of numerical instability. The spectra have been generated as follows. Fluctuations of velocity were recorded over a sufficiently long time interval at 20 equispaced stations along the streamwise direction. Each station had several probing points, so that the spectrum at a given station is actually averaged in the cross-flow direction. Averaging is performed after a power spectral density (PSD) distribution is obtained for each of the probing points in a section. Fig. 5 shows PSD curves of the cross-flow velocity vs. angular frequency ω (scaled by h/p) for the 20 streamwise stations. As a unit mean velocity has been used, ω can also be regarded as a streamwise wavenumber k via Taylor's frozen flow hypothesis. The vertical dashed lines in Fig. 5 mark $kh/P = 3$ which is estimated from Fig. 3 to be the wavenumber after which dissipation becomes significant.

Linear dispersion-diffusion analysis is again relied upon as a source of insight on accuracy and robustness. We consider spectral vanishing viscosity (SVV) as a possible stabilization technique. SVV can be regarded as a modified diffusion operator that damps mainly high-order polynomial coefficients (a low-pass filter). Fig. 3 shows absolute values of CG's numerical dissipation for linear advection with and without SVV. Two propagation modes exist in each case, a regular one (physical) and a spurious one related to reflected waves. The latter originate when mesh spacing varies and can actually be seen in Fig. 4 as noise slowly dissipated upstream of station 60%. Without SVV, regular and reflected modes coincide and there is nearly zero damping for the reflected mode for a large wavenumber range. SVV damps considerably the reflected waves, but also affects the physical ones by shortening the dissipation-free range.

The energy pile-up observed in Fig. 5 is believed to be caused by a non-linear interaction between incoming vortical structures and the reflected noise, as if it was a forcing mechanism causing 'turbulence' to grow. While SVV reduces the noise and stabilizes simulations, it also damps small scales otherwise captured. Hence, it is hard to know a priori the ideal amount of SVV to be added – note that Fig. 3 is just a representative example since SVV has several design parameters. An alternative is to tune SVV diffusion levels to match those of standard upwind DG. This has been done by Moura *et al.* (2016*b*) for temporally evolving problems, but only more recently extended to spatially developing flows. This latter extension is discussed here for the first time. The key principle is to optimize SVV's parameters so as to match the slope of DG's dissipation curves in log-log plots. Due to DG's superconvergence properties (Hu & Atkins, 2002) manifested near the origin of those plots, it was impossible to match same-order discretizations. This motivated us to match CG order p to DG order $p-2$. Excellent matching was achieved for CG with $p = 3, \ldots, 10$. The resulting CG discretizations were found to be very robust. For the vortical flows under consideration, computations remained stable regardless of the Reynolds number, even in essentially inviscid cases. These even matched (visually) flow fields produced by inviscid DG-based cases (of order $p-2$).

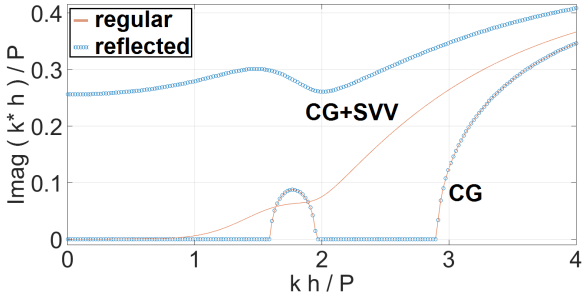

Figure 3. CG's dissipation with and without SVV.

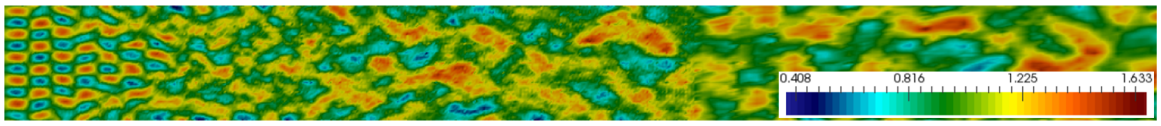

Figure 4. Streamwise velocity contours in 2D vortical flow. Streamwise mesh spacing increases after 60% of domain length.

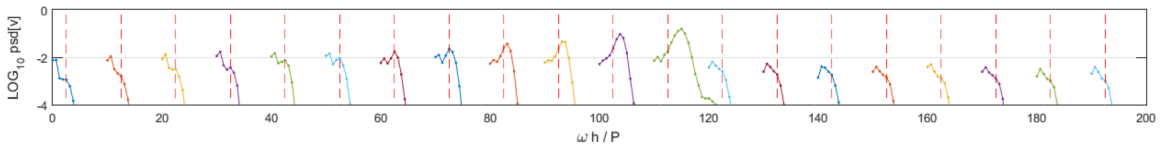

Figure 5. Power spectral density of crossflow velocity at different sections along the streamwise direction. Energy pile-up is observed just before the change in streamwise mesh spacing. Curves have been shifted horizontally by ten units each for clarity.

An additional constraint in the optimization process made sure that dissipation levels of the spurious (reflected) eigenmodes were always above a given threshold — causing spurious reflections to be practically eliminated in the test cases. Also, as a natural outcome of the optimization strategy, premature dissipative "bumps" (cf. Fig. 3) were slightly overcome due to the target dissipation levels adopted. This resulted in strictly monotonic dissipation curves, preventing potentially undesirable non-smooth dissipative features. A drawback of the proposed strategy is that relatively large dissipation is assigned to lower-order discretizations, especially $p = 3$, which had a clearly reduced resolution power for the model problem considered. However, increasing p does recovered good resolution power per DOF, as happens with DG.

TRANSITIONAL / TURBULENT FLOWS IN 3D

In this section we discuss DG-based solutions of the inviscid and (nearly) incompressible Taylor-Green vortex (TGV) flow (Shu *et al.*, 2005). This is a model problem featuring transition and turbulence decay in a triply-periodic domain that extremely demanding in terms of numerical robustness. The Euler equations have been solved directly with Mach = 0.1, but the presence of numerical viscosity is expected to make solutions consistent with the dissipative behaviour of infinite Reynolds number. In comparison to traditional LES, this scenario corresponds to that where molecular viscosity effects are negligible and a subgrid-scale model acts alone.

An extensive set of test cases have been conducted for various polynomial orders ($p = 3, \ldots, 7$) on different grids of cubic-shaped elements. This allowed for an assessment of DG's performance for uDNS of free transitional / turbulent flows at very high Reynolds numbers on a fixed DOF basis. Different Riemann fluxes have also been tested, in particular Roe and Lax-Friedrichs (also called Rusanov) solvers (Toro, 1999). These are arguably the most common fluxes used in conjunction with high-order DG nowadays. More details about these computations and a complete discussion of results can be found in (Moura *et al.*, 2017). The main goal of that study was to validate in actual 3D turbulent flows the criterion proposed in (Moura *et al.*, 2015*b*) to estimate DG's resolution power, namely the so-called "1% rule". This rule differentiates wavenumber ranges of negligible and significant dissipation for various polynomial orders (recall Fig. 1) by assuming a threshold of 1% damping factor per DOF crossed by travelling waves. From this threshold, one is able to evaluate the wavenumber $k_{1\%}$ beyond which numerical diffusion becomes significant enough to induce a dissipation range on the energy spectra of DG-uDNS. The concept is closely related to that of eddy-resolving capability and (implicit) LES filter width.

A simple adaptation to the 1% rule is however needed from 1D to 3D settings, owing to how energy spectra are defined in 3D, see (Moura *et al.*, 2017) for more details. This essentially causes the numerically-induced dissipation range of 3D spectra to begin in between $k_{1\%}$ and $\sqrt{3}k_{1\%}$. This adaptation worked very well for Roe-based test cases and reasonably well for those cases based on Lax-Friedrichs, as shown in Fig. 6. Note that the so-called complete solvers (which treat all the eigenvalues of governing equations' system consistently) yielded results similar to Roe, whereas incomplete ones performed like Lax-Friedrichs. The latter displayed a delay in the onset of their dissipation range due to an unphysical pile-up of small-scale energy seen as an "energy bump" before the actual dissipation range. Also, they have less energy in the intermediate scales when compared to Roe-based solutions, causing Kolmogorov's $-5/3$ slope to be followed over a reduced wavenumber range at TGV's dissipation peak ($t \approx 9$).

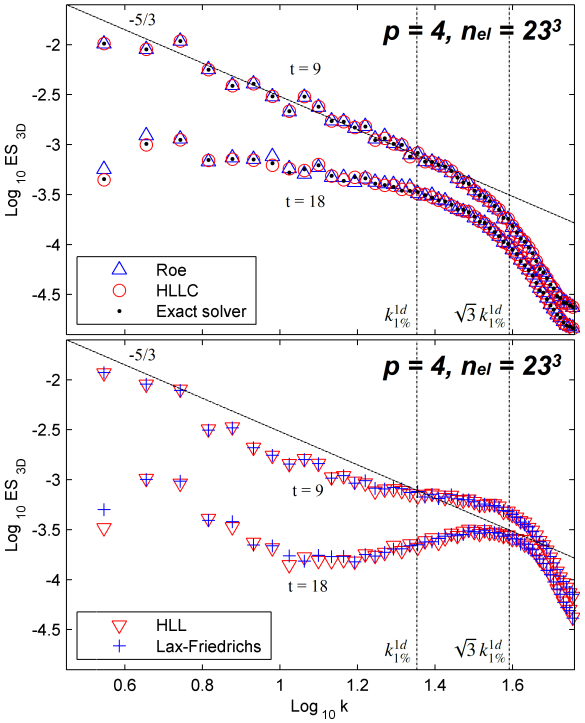

Figure 6. Energy spectra of the inviscid TGV flow at $t = 9$ (dissipation peak) and $t = 18$ for various Riemann solvers.

A visual comparison between the flow fields generated by Roe and Lax-Friedrichs is given in Fig. 7, which clearly shows how energy bumps are connected to over-energetic small-scale spurious structures. Energy bumps have also been observed in turbulence computations when hyperviscosity is used in place of the regular (2nd-order) diffusion operator (Lamorgese *et al.*, 2005), and they

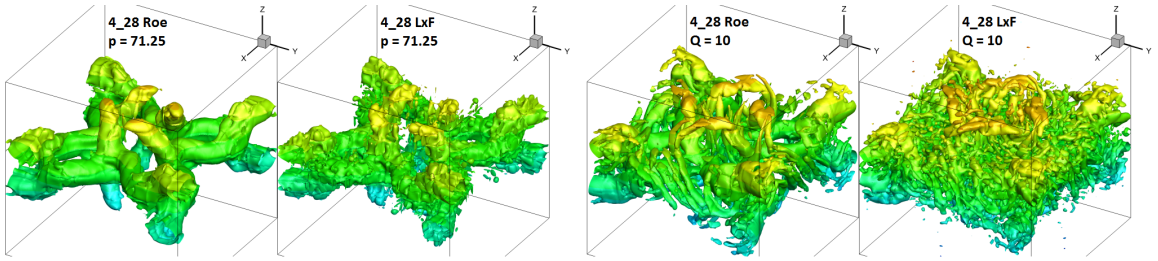

Figure 7. Isosurfaces of pressure (left pair) and Q-criterion (right pair) comparing cases based on Roe (cleaner) and Lax-Friedrichs (noisier). Results obtained with $p = 3$ and $n_{el} = 28^3$ at $t = 7$. Only one-eighth of the domain is shown; isosurfaces coloured by height (z-coordinate).

are seen to grow when the hyperviscous exponent increases. This is explained as a stronger bottleneck phenomenon (Falkovich, 1994) taking place due to a sharper dissipative behaviour in wavenumber space. Reduced energy levels prior to energy bumps have also been observed in numerical experiments conducted with hyperviscosity and result from an intense eddy viscosity-like mixing effect caused by the over-energetic small scales (Frisch *et al.*, 2008). We note that the Lax-Friedrichs flux is also expected to yield a sharper dissipation in Fourier space owing to its over-upwind bias at low Mach numbers, as explained below.

The standard upwind conditions is best represented by Roe's formula, which employs a property jump term proportional to the corresponding eigenvalues of the governing equations' system. On the other hand, the Lax-Friedrichs flux uses instead the eigenvalue of maximum absolute value alone. In 1D, for example, the latter solver replaces $|u|$ with $|u|+c$ in the momentum equations, where u is the flow velocity and c is the speed of sound. This amounts to an over-upwinding factor of $\beta = (|u|+c)/|u| = 1+\mathrm{Mach}^{-1}$, which increases without bound as the Mach number is reduced. Fig. 8 illustrates DG's dissipation eigencurve for three ratios β when $p = 4$. As the Mach number decreases, a discontinuity appears on the curve. Moreover, for case $p = 4$ shown, the magnitude of the discontinuous variation increases about twelve times as Mach is reduced from 0.9 to 0.1. These results are to be contrasted with those obtained with standard upwinding (Fig. 1) which represent Roe-type solvers and do not depend on the Mach number.

An additional assessment of solution quality is made by the so-called QR diagrams (Chong *et al.*, 1990; Tsinober, 2009). These will further illustrate how physical or unphysical DG-uDNS results can be for the type of problem considered in this section. QR diagrams, cf. Fig. 9, consist of joint PDFs of the second (Q) and third (R) invariants of the velocity gradient tensor for a given flow field (Chong *et al.*, 1990) and provide a statistical description of turbulent kinematics. The teardrop-like profile shown for the Roe case in Fig. 9 (top) is also observed in several different turbulent flows, see e.g. (Laizet *et al.*, 2015), and is regarded as one of the qualitatively universal characteristics of turbulence (Tsinober, 2009). On the other hand, profiles obtained from Lax-Friedrichs computations yielded a more symmetrical distribution of kinematic states, typical of artificially generated Gaussian turbulence (Chertkov *et al.*, 1999). This symmetric distribution is possibly associated to the energy bump discussed previously, as bump-related scales represent a so-called thermalized state (Banerjee & Ray, 2014) where energy equipartition is favoured (Frisch *et al.*, 2008).

At this point, it is important to note that some of the TGV test cases considered lacked numerical stability and "crashed", normally before the problem's kinetic energy dissipation peak was achieved ($t \approx 9$). This happened especially at higher polynomial orders ($p \geq 5$), which is not surprising since high-order numerical schemes (in general) usually have very low dissipation. However, Roe-based computations crashed less often and, depending on the grid, remained stable even at $p = 8$. Lax-Friedrichs, on the other hand, offered less robustness and crashed for $p \geq 5$ on all grids tested. This is considered counter-intuitive since that latter is usually regarded as more dissipative and hence more stable. It is believed, therefore, that the observed instabilities are not caused by insufficient dissipation, but by a sharper dissipative behaviour in wavenumber space. Lax-Friedrichs does exacerbate this behaviour due to its over-upwind bias at low Mach numbers, but higher order discretizations also produce sharper dissipation even at standard upwind conditions (Fig. 1). It so happens that very sharp dissipation curves can induce a partial shift from a dissipative to a conservative flow dynamics (Frisch *et al.*, 2008; Banerjee & Ray, 2014), whereby physical instabilities can arise in the inviscid TGV flow, although the possibility of physical TGV singularities leading to solution collapse is still under debate (Brachet *et al.*, 1992; Cichowlas & Brachet, 2005; Hou & Li, 2008).

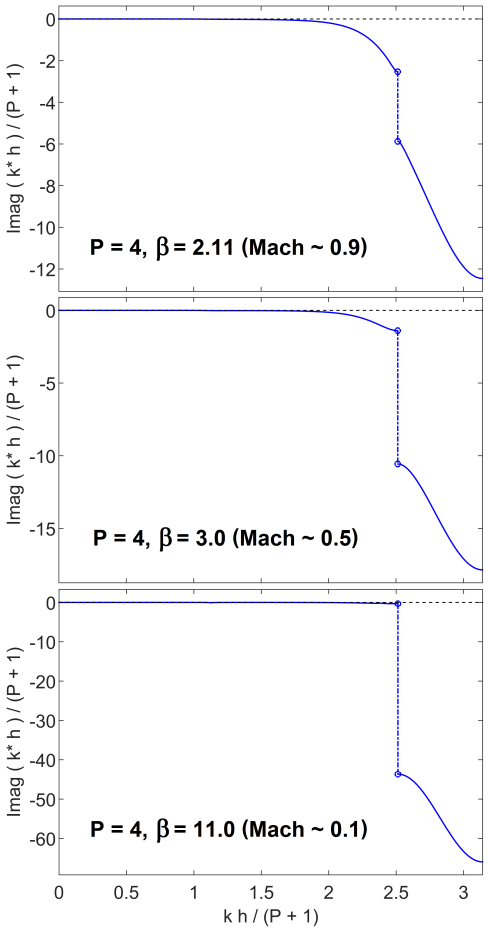

Figure 8. Lax-Friedrichs' dissipation curves for $p = 4$ and Mach number 0.9 to 0.1 (top to bottom). Plot from (Moura *et al.*, 2016*a*).

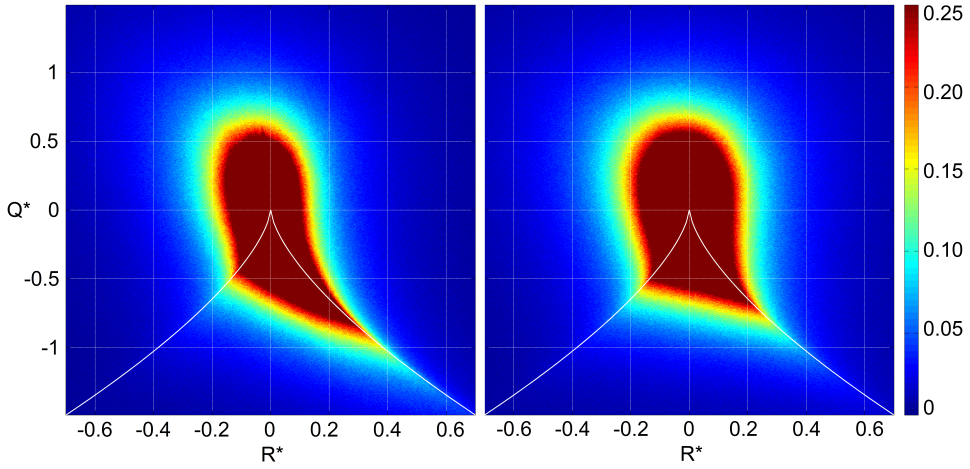

Figure 9. QR diagrams at $t = 9$ (dissipation peak) obtained with Roe (left) and Lax-Friedrichs (right), from case $p = 4$, $n_{el} = 23^3$. The dark red colour has been assigned to values above $1/4$. The white curve separates rotational states (above the curve) from those without rotation (under the curve), cf. (Chong *et al.*, 1990).

The lack of robustness for the higher-order discretisations has been cautiously verified not to be related with time-step restrictions or polynomial aliasing errors. Typical CFL numbers (based on the acoustic wave speed) were of the order of 10^{-1} and an increased number of quadrature points ($q = 2m$ per dimension) has been employed in all the cases to ensure consistent integration of the cubic non-linearities of the compressible Euler equations. Tests conducted with particular cases to rule out these factors consistently showed the time of crash to be insensitive to time-step reductions (down to CFL $\approx 10^{-2}$) or to a further increase in the number of integration points (up to $q = 4m$). The 'global dealiasing' approach described in Mengaldo *et al.* (2015) has been employed for the interior and boundary quadratures, where over-integration is performed simply through a larger number of (Gauss-Lobatto-Legendre) quadrature points. The unstable simulations obtained highlight that DG-based uDNS approaches, even with consistent/over-integration, might in fact require additional stabilization techniques at very high Reynolds numbers so as to more strongly enforce the entropy-consistent dissipative behaviour of Navier-Stokes turbulence in the limit of zero viscosity.

Finally, a skew-symmetric (or split-form) DG formulation recently proposed (Gassner *et al.*, 2016) was able to stabilize all the TGV test cases considered here and others, up to order 16th, without significantly impacting DG's resolution power (Winters *et al.*, 2017). Such approach is very robust and, when used with complete Riemann solvers, a promising candidate for high-fidelity practical applications. Further investigation is however still required for DG-uDNS in different types of flows and especially for wall-bounded turbulence.

CONCLUSIONS

This study investigated the suitability of high-order spectral element methods (SEM), in particular the continuous and discontinuous Galerkin methods (i.e. CG and DG), to under-resolved DNS (uDNS) / implicit LES (iLES). Model problems in 1D, 2D and 3D have been covered, each providing peculiar insight into the accuracy and stability of CG- or DG-based uDNS / iLES. Results obtained from numerical experiments have been explained according to linear dispersion-diffusion (eigen)analysis. One of the main insights stemming from the eigenanalysis concerned the estimation of DG's resolution power or eddy-resolving capability. Numerical results also demonstrated that DG approaches have superior robustness due to their inherent upwind dissipation, whereas CG requires added spectral vanishing viscosity (SVV) to remain stable at high Reynolds numbers. A viable approach to design SVV operators suited to under-resolved computations is to match SVV dissipation levels to those of DG.

The results obtained with DG for the Taylor-Green vortex (TGV) problem at infinite Reynolds number highlighted that, when the effects of molecular viscosity are negligible, "complete" Riemann solvers (such as Roe's flux) and moderately high polynomial orders should be favoured. This is to avoid unphysical results induced by very sharp dissipative behaviour in wavenumber space, caused either by very high polynomial orders or by the over-upwinding bias of more simplistic solvers (such as Lax-Friedrichs). For spatially developing problems, using complete Riemann solvers also helps to suppress spurious reflections (Hu & Atkins, 2002), which is also expected to improve numerical stability (Mengaldo *et al.*, 2017).

A final requirement for robustness is the mitigation of polynomial aliasing errors caused by insufficient quadratures (Mengaldo *et al.*, 2015). For CG, dealiasing is more easily performed due to the reduced (quadratic) nonlinearity of the incompressible Navier-Stokes equations (Kirby & Karniadakis, 2003). We note that CG is almost exclusively used for incompressible flows, whereas discontinuous SEM are much more often employed for compressible ones. As a result, dealiasing for DG is more involved and expensive since the conservative form of the compressible Navier-Stokes equations has rational terms which are hardly integrated exactly in under-resolved scenarios. Although quadratures with an increased number of integration points can be performed, these can be eventually ineffective in suppressing instabilities due to under-resolution at very high Reynolds (as shown in the TGV cases discussed).

A recently proposed skew-symmetric (or split-form) DG discretization (Gassner *et al.*, 2016) demonstrated remarkable numerical stability by being able to stabilize inviscid TGV computations even at very high order. This approach is a promising candidate for high-fidelity uDNS / iLES of practical flows. Still, further investigation is required regarding the suitability of high-order SEM for different types of transitional and turbulent flows, especially for wall-bounded flows and complex geometries.

REFERENCES

Banerjee, D. & Ray, S. S. 2014 Transition from dissipative to conservative dynamics in equations of hydrodynamics. *Phys. Rev. E* **90** (4), 041001.

Beck, A. D., Bolemann, T., Flad, D., Frank, H., Gassner, G. J., Hindenlang, F. & Munz, C. D. 2014 High-order discontinuous Galerkin spectral element methods for transitional and turbulent flow simulations. *Int. J. Numer. Meth. Fl.* **76** (8), 522–548.

Brachet, M. E., Meneguzzi, M., Vincent, A., Politano, H. & Sulem, P. L. 1992 Numerical evidence of smooth self-similar dynamics and possibility of subsequent collapse for three-dimensional ideal flows. *Phys. Fluids A* **4** (12), 2845–2854.

Chertkov, M., Pumir, A. & Shraiman, B. I. 1999 Lagrangian tetrad dynamics and the phenomenology of turbulence. *Phys. Fluids* **11** (8), 2394–2410.

Chong, M. S., Perry, A. E. & Cantwell, B. J. 1990 A general classification of three-dimensional flow fields. *Phys. Fluids A* **2** (5), 765–777.

Cichowlas, C. & Brachet, M.-E. 2005 Evolution of complex singularities in Kida–Pelz and Taylor–Green inviscid flows. *Fluid Dyn. Res.* **36** (4), 239–248.

Dairay, T., Lamballais, E., Laizet, S. & Vassilicos, J. C. 2017 Numerical dissipation vs. subgrid-scale modelling for large eddy simulation. *J. Comput. Phys.* **337**, 252–274.

Falkovich, G. 1994 Bottleneck phenomenon in developed turbulence. *Phys. Fluids* **6** (4), 1411.

Fernandez, P., Nguyen, N. C. & Peraire, J. 2017 The hybridized Discontinuous Galerkin method for Implicit Large-Eddy Simulation of transitional turbulent flows. *J. Comput. Phys.* **336**, 308–329.

Frisch, U., Kurien, S., Pandit, R., Pauls, W., Ray, S. S., Wirth, A. & Zhu, J. Z. 2008 Hyperviscosity, Galerkin truncation, and bottlenecks in turbulence. *Phys. Rev. Lett.* **101** (14), 144501.

Gassner, G. J. & Beck, A. D. 2013 On the accuracy of high-order discretizations for underresolved turbulence simulations. *Theor. Comp. Fluid Dyn.* **27** (3-4), 221–237.

Gassner, G. J., Winters, A. R. & Kopriva, D. A. 2016 Split form nodal discontinuous Galerkin schemes with summation-by-parts property for the compressible Euler equations. *J. Comput. Phys.* **327**, 39–66.

Grinstein, F. F., Margolin, L. G. & Rider, W. J. 2007 *Implicit large eddy simulation: computing turbulent fluid dynamics*. Cambridge University Press.

Hou, T. Y. & Li, R. 2008 Blowup or no blowup? The interplay between theory and numerics. *Physica D* **237** (14), 1937–1944.

Hu, F. Q. & Atkins, H. L. 2002 Eigensolution analysis of the discontinuous Galerkin method with nonuniform grids. *J. Comput. Phys.* **182** (2), 516–545.

Kirby, R. M. & Karniadakis, G. E. 2003 De-aliasing on non-uniform grids: algorithms and applications. *J. Comput. Phys.* **191** (1), 249–264.

Laizet, S., Nedić, J. & Vassilicos, C. 2015 Influence of the spatial resolution on fine-scale features in DNS of turbulence generated by a single square grid. *Theor. Comp. Fluid Dyn.* **29** (3-5), 286–302.

Lamballais, E., Fortuné, V. & Laizet, S. 2011 Straightforward high-order numerical dissipation via the viscous term for direct and large eddy simulation. *J. Comput. Phys.* **230** (9), 3270–3275.

Lamorgese, A. G., Caughey, D. A. & Pope, S. B. 2005 Direct numerical simulation of homogeneous turbulence with hyperviscosity. *Phys. Fluids* **17** (1), 015106.

Lombard, J.-E. W., Moxey, D., Sherwin, S. J., Hoessler, J. F. A., Dhandapani, S. & Taylor, M. J. 2016 Implicit large–eddy simulation of a wingtip vortex. *AIAA J.* **54** (2), 506–518.

Margolin, L.G. & Rider, W.J. 2002 A rationale for implicit turbulence modelling. *Int. J. Numer. Meth. Fl.* **39** (9), 821–841.

Margolin, L.G. & Rider, W.J. 2005 The design and construction of implicit LES models. *Int. J. Numer. Meth. Fl.* **47** (10-11), 1173–1179.

Mengaldo, G., De Grazia, D., Moxey, D., Vincent, P. E. & Sherwin, S. J. 2015 Dealiasing techniques for high-order spectral element methods on regular and irregular grids. *J. Comput. Phys.* **299**, 56–81.

Mengaldo, G., Moura, R. C., Giralda, B., Peiró, J. & Sherwin, S. J. 2017 Spatial eigensolution analysis of discontinuous Galerkin schemes with practical insights for under-resolved computations and implicit LES. *Comput. Fluids (submitted)* .

Moura, R.C., Mengaldo, G., Peiró, J. & Sherwin, S.J. 2016*a* An LES setting for DG-based implicit LES with insights on dissipation and robustness. In *Proceedings of the 11th International Conference on Spectral and High Order Methods (under review)*. Rio de Janeiro, Brazil.

Moura, R.C., Sherwin, S.J. & Peiró, J. 2015*a* Modified equation analysis for the discontinuous Galerkin formulation. In *Spectral and High Order Methods for PDEs – ICOSAHOM 2014*, pp. 375–383. Springer.

Moura, R. C., Mengaldo, G., Peiró, J. & Sherwin, S. J. 2017 On the eddy-resolving capability of high-order discontinuous Galerkin approaches to implicit LES / under-resolved DNS of Euler turbulence. *J. Comput. Phys.* **330**, 615–623.

Moura, R. C., Sherwin, S. J. & Peiró, J. 2015*b* Linear dispersion-diffusion analysis and its application to under-resolved turbulence simulations using discontinuous Galerkin spectral/*hp* methods. *J. Comput. Phys.* **298**, 695–710.

Moura, R. C., Sherwin, S. J. & Peiró, J. 2016*b* Eigensolution analysis of spectral/*hp* continuous Galerkin approximations to advection-diffusion problems: insights into spectral vanishing viscosity. *J. Comput. Phys.* **307**, 401–422.

Shu, C. W., Don, W. S., Gottlieb, D., Schilling, O. & Jameson, L. 2005 Numerical convergence study of nearly incompressible, inviscid Taylor–Green vortex flow. *J. Sci. Comput.* **24** (1), 1–27.

Toro, E. F. 1999 *Riemann solvers and numerical methods for fluid dynamics*. Springer.

Tsinober, A. 2009 *An informal conceptual introduction to turbulence*, , vol. 483. Springer.

Uranga, A., Persson, P. O., Drela, M. & Peraire, J. 2011 Implicit large eddy simulation of transition to turbulence at low Reynolds numbers using a discontinuous Galerkin method. *Int. J. Numer. Meth. Eng.* **87** (1-5), 232–261.

Vermeire, B. C., Nadarajah, S. & Tucker, P. G. 2016 Implicit large eddy simulation using the high-order correction procedure via reconstruction scheme. *Int. J. Numer. Meth. Fl.* **82** (5), 231–260.

Winters, A. R., Moura, R. C., Mengaldo, G., Gassner, G. J., Walch, S., Peiró, J. & Sherwin, S. J. 2017 A comparative study on polynomial dealiasing and split form discontinuous Galerkin schemes for under-resolved turbulence computations. *Comput. Method. Appl. M. (submitted)* .